Renewable Energy 101 (2017) 1169–1179

Contents lists available at ScienceDirect

Renewable Energy

journal homepage: www.elsevier.com/locate/renene

Spectral characterization of the solar resource of a sunny inland site for flat plate and concentrating PV systems

R. García, M. Torres-Ramírez, E. Muñoz-Cerón, J. de la Casa, J. Aguilera*

IDEA Research Group, University of Jaén, Campus de Las Lagunillas, 23071, Jaén, Spain

ARTICLE INFO

Article history:
Received 11 May 2016
Received in revised form
20 September 2016
Accepted 24 September 2016

Keywords:
Solar radiation
Spectral irradiance distribution
Average photon energy
PV technologies

ABSTRACT

The spectrum is not frequently used when rating any PV technology. Moreover, in those energy predictions where it is considered, normally they are based on simulated models. The objective of this work is the spectral characterization of the solar resource based on real measurements as their availability in the scientific community is scarce.

For this characterization the Average Photon Energy is used, which has been obtained from an experimental campaign carried out in Jaén (Spain) based on three different configurations: Direct Normal spectrum (DNI tracker), Global spectrum on a tracking system (GI tracker) and Global spectrum on a fixed surface (GI fixed).

The results show that the annual irradiance weighted average value of APE results in 1.80 eV for DNI tracker, 1.85 eV for GI tracker and 1.86 eV for GI fixed, showing a red spectral shift for the DNI measurements.

A Red-rich spectrum prevails, so this location is especially suitable for single junction materials with a large absorption band such as CIGS and c-Si. Besides, GI tracker spectra are slightly redder than GI fixed ones, consequently, if c-Si modules are used, spectral gains with 2-axis tracking will be higher than those achieved with a fixed arrangement of such modules.

1. Introduction

One of the main inputs for the characterization of many engineering energy projects is the solar radiation. Among them, Photovoltaic (PV) and Concentrated Solar Power (CSP) technologies are the most important ones in taking advantage of the solar resource [1,2]. In this sense, the identification of the optimal location to maximize the radiation captures is a key aspect when planning these solar projects. Therefore, the information related to the solar resource is a basic requirement in the design stage in order to estimate its influence in the energy generation predictions.

Focusing on the photovoltaic technology it is sufficient well-known the influence of the solar irradiance and module temperature in their operation under outdoor real conditions [3–5]. These variables contribute to the differences of performance of PV devices in each location. In this sense, a prior evaluation of these environmental factors in order to assess the suitability of the location selected is an essential requirement to ensure the feasibility of a photovoltaic project.

Particularly important among the variables that define the solar resource, which it is not so deeply and widely analysed, is the spectral distribution as it has a remarkable influence on the performance of certain photovoltaic technologies. Thin-film (e.g. single-junction amorphous Si, CdTe, CIGS, and double-junction “micromorph” Si), concentrating photovoltaic (CPV) or the newest trend such as perovskite solar cells are the PV technologies most influenced by the solar spectrum distribution [6–9]. The peculiarities of the spectral responses of the aforementioned technologies imply that they are more sensitive to the shape of the solar spectrum, that is, its distribution, than other traditional PV technologies based on crystalline silicon. Therefore, besides the module temperature and in addition to the solar irradiance values available on the module's surface, the spectrum shape must be taken into account when modelling and rating the power output of certain PV technologies.

In this sense, proven and real information related to the solar resource -irradiance and spectral distribution-of a certain location

* Corresponding author.
E-mail address: aguilera@ujaen.es (J. Aguilera).

http://dx.doi.org/10.1016/j.renene.2016.09.060
0960-1481/

is a basic data input for the analysis of the performance of these PV technologies. However, spectral irradiance measurements needed to assess and quantify the spectral influence on the outdoor performance of the solar modules are rarely available in meteorological stations worldwide. Due to this scarcity of real data, in order to estimate the spectral dependency in the output performance of certain PV technologies, some models have been developed to simulate and replicate the spectral distribution of irradiance of selected areas. Most common software tools and applications which are used for this simulated models are: SMARTS2, SEDES2, SBDART, MODTRANS, ASPIRE and RRTM SW [10–14]. Besides, models which simulates the spectral characteristics of diffuse light have been also developed [15,16]. Additionally, a novel model based on artificial intelligence techniques has been also applied in this field with promising and successful results [17]. Apart from the scarcity of measured data collected by means of spectroradiometers, the format of their data output are not easily applicable to simple modelling or for engineering approaches. These data consist on a set of points together with a wavelength interval, namely one-dimensional data, which depends on the spectral range and the instrument's resolution.

The use of the entire solar spectrum range has some drawbacks, so in order to deal with these data statistically and characterize the solar spectrum, a non-dimensional variable is necessary. Previous scientific papers have used different parameters such as the Useful Fraction (UF) [18], defined as the proportion of global radiation that falls within the acceptance window of a particular measurement device. Nevertheless, UF is device dependent from the PV technology under investigation and therefore it has to be recalculated for each different type of device used. Another parameter frequently used is the Average Photon Energy (APE), which was proposed by Gottschalg's group of Loughborough University [19]. APE is a single value that depends on the shape of the incident irradiance spectrum but not on its intensity. This index averages energetically a solar spectral distribution to a mean value, so the advantage is its independency from the PV technology used. This index is the one used in this paper and it is calculated dividing the incident irradiance by the total photon flux density:

$$APE = \frac{\int_{\lambda_1}^{\lambda_2} E_\lambda(\lambda)\cdot d\lambda}{\int_{\lambda_1}^{\lambda_2} \phi(\lambda)\cdot d\lambda} \quad (1)$$

Where $E_\lambda(\lambda)$ [W m^{-2} μm^{-1}] is the spectral in-plane irradiance, $\Phi(\lambda)$ [m^{-2} μm^{-1} s^{-1}] is the spectral photon flux density, λ_1 [nm] and λ_2 [nm] are the lower and upper wavelength limits, respectively, of the considered interval of the solar spectrum to be measured. The values for the wavelength interval are usually determined by the measurement range of the spectroradiometer.

The most suitable wavelength range for the APE calculation would be the full terrestrial spectrum (280–4000 nm), thus resulting in the true APE value. However, it is difficult to find instruments which measure the whole range. The majority of the most extended commercial spectroradiometers usually measure within the wavelength range of 350–1050 nm. For some specific spectral characterization, smaller intervals of the most important part of the spectrum are measured, which most of the times corresponds to the region with higher spectral irradiance, and thereafter, the spectrum is extended using some of the aforementioned mathematical models. This procedure results in a reasonable accuracy [20,21]. Likewise previous scientific papers which cover this wavelength range, for this work it has also be chosen.

In order to classify each spectrum obtained, the reference solar spectral irradiance distribution AM 1.5 is used in this document as it provides a common reference for the evaluation of PV devices [22,23]. Differentiating between the global and direct radiation data, the APE value changes from 1.85 eV for the AM 1.5 direct (AM 1.5D) standard solar spectrum while for the global distribution, AM 1.5G, its value is 1.88 eV [24,25]. In both cases, these values were calculated in the wavelength range of 350–1050 nm.

In previous papers, various authors have studied the spectral irradiance using APE as indicator and its influence in different PV technologies, such as Gottschalg et al. in Loughborough (UK) [19,26], Cornaro and Andreotti in Rome (Italy) [27], Minemoto et al. in Kusatsu City (Japan) [3,28], Chattariya S et al. in Phitsanulok (Thailand) [4] and Dirnberger D et al. in Freiburg im Breisgau (Germany) [7], among others. Some of them have assured that APE has an unique value for each possible solar distribution [24,27]. Nevertheless, this assumption has been questioned by Gueymard and other authors [7,29,30]. These authors conclude that relating the PV performance solely to the APE and the module temperature is a flawed approach and it requires further investigation. Despite this lack of scientific agreement, it is clear that the APE is a meaningful and suitable index to ascertain the influence of the solar spectrum on PV performance [4,27,28,31]. As a general overview, the higher the APE, the richer in blue content the solar light is; in other words, high values of APE lead to enhanced shorter wavelengths of the solar spectrum.

However, as it was stated before, real spectral measurements are scarcely addressed in most meteorological stations, databases and papers, which leads to the situation where real spectral effects are either simulated or even not considered. Thus, in sunny inland climates there is a lack of spectral measurements and availability of APE values [31]. Moreover, previous research papers published have focused on the influence of the spectral distribution and the APE calculation in different PV technologies performance, but none of them have extended this study to the tracking mechanism used.

Therefore, this paper overcomes the scarcity of real measured data and it provides knowledge about the typical spectral characteristics in this type of climate differentiating between fix or tracking options, which may be useful for the performance estimations of flat plate and CPV systems.

2. Purpose of the work

This paper analyses the spectral distribution differences depending on the tracking mechanism considered in the PV system. The assessment of these differences is made by means of the APE calculation through real measurements of solar irradiation and spectral data. A detailed study was carried out during a complete year in order to evaluate and compare these differences according to spectral irradiance measurements in a site with sunny inland climate. Specifically, the following variables have been measured and compared:

1. Direct Normal solar spectrum on a 2-axis tracking system, which will be identified as “DNI tracker” from now on.
2. Global solar spectrum on a 2-axis tracking system, identified as “GI tracker”.
3. Global solar spectrum on a fixed south facing tilted surface, denominated “GI fixed” in this document.

None of the tracking mechanisms are unknown to the scientific community. However, recent papers found in the PV literature have shown the importance of considering the solar spectrum impinging on these surfaces in order to improve the accuracy of the energy forecasting methods of PV systems [3,4,19,26,27]. Particularly, several studies have revealed the lack of supporting

studies which use empirical spectral irradiance measurements [17,26,27]. Therefore, this work provides large amount of meaningful real outdoors data to analyse the solar spectrum peculiarities according to the tracking options considered for the specified location. Due to the fact that no similar comparative spectral characterization of a site with sunny inland climate based on real data has been previously addressed, this paper can be very clarifying and useful for further scientific works and even for the CPV and Thin-Film industry.

This paper is organized as follows: initially, the experimental setup and the applied methodology are detailed in Section 3 where the tested tracking options used to analyse the differences in terms of spectral irradiance are also described. Subsequently, the results and their further discussion are discussed in Section 4, where a comparative study dealing with outdoor spectral characterizations has been carried out. Some statistical parameters are used to assess the dissimilarities of the tracking options analysed. Finally, the conclusions and future works are summarized in Section 5.

3. Materials and methods

This paper proposes an evaluation of the spectral irradiance distribution based on three different tracking options (DNI tracker, GI tracker and GI fixed). For that purpose, data have been collected and analysed over a 12-month experimental campaign for each tracking mechanism. These measurements were carried out outdoors at Jaén (Southern Spain) on the following periods: from November 2011 to October 2012 for the GI tracker option, from January 2012 to December 2012 for GI fixed measurements and finally, from March 2013 to February 2014 for DNI tracker. Figs. 1 and 2 show the equipment used for each of the options analysed.

The data recorded during these periods have provided a large amount of meaningful information to set a solid basis which allows us to analyse the differences in term of spectral irradiance distribution in a sunny inland location. These real measured samples are used to establish a comparative study according to a spectral characterization of the selected site. Finally, the divergences between the measured spectral irradiance distributions regarding the three tracking options were quantified.

3.1. Experimental setup and outdoors campaign

The experiment was carried out for a complete meteorological year in the city of Jaén, located in Southern Spain. Table 1 [32] shows some relevant climatological information regarding the selected location.

Measurements have been carried out using an automatic experimental set-up, which has been designed and implemented by the Research and Development in Solar Energy (IDEA) Group of the University of Jaén. This test and measurement system has been previously described and successfully used in other research experiments [33,34].

The spectroradiometers used for this study were mounted on three different tracking configurations: namely, the first tracking option was tested with the purpose of registering the spectral distribution of the Direct Normal Irradiance impinging on a two-axes tracking surface (DNI tracker), whereas the last two tracking configurations (GI tracker and GI fixed) are related to the spectral distribution of the Global Irradiance impinging on a two-axes tracking surface and a fixed tilted structure, respectively. In particular, the GI fixed spectroradiometer was coplanar mounted to a South-facing structure with a tilt angle of 36°. This tilt angle selected was meant to maximize the annual irradiation collection. This criterion is widely followed when designing PV grid-connected systems, provided that no constraints such as those imposed by architectural integration prevent the PV designer from following it. Assuming no constrains at all, the optimal tilt angle for Madrid (Spain, latitude 40°24′N, longitude 3°42′W) lies precisely at 36° [35,36]. This value may be assumed as well for Jaén (Spain, latitude 37°45′N, longitude 3°47′) with no significant error. The other spectroradiometer was coplanar mounted to a precise two-axis solar tracker. The data acquisition system required to capture all data was located on the roof of the Polytechnic School of the Engineering building at the University of Jaén. This equipment was placed on a shadow-free horizontal surface and readily accessible for inspection and general cleaning. All spectroradiometers, pyrheliometer and pyranometers were periodically cleaned to avoid soiling.

Fig. 1. Experimental setup for DNI and GI tracker option.

In this study the Global Irradiance (G), *the DNI* and E_λ were measured by means of a pyranometer, a pyrheliometer and three spectroradiometers respectively. These meteorological data were recorded at 5-min time intervals during 12 months for each tracking option between Nov-2011 and Feb-2014. It should be mentioned that G and *DNI* are measured by means of a Kipp&Zonen™ CMP21 pyranometer and a Kipp&Zonnen CHP 1 pyrheliometer, respectively, whereas, in order to register the spectral irradiance distribution (E_λ), three EKO™ MS700 spectroradiometers were used. The spectral irradiance distribution has

Fig. 2. Measurement devices for GI fixed option.

Table 1
Annual average figures of some relevant meteorological parameters recorded in Jaén over 30 years [32].

Horizontal irradiation (kWh m^{-2})	T_{amb} (°C)	Minimum T_{amb} (°C)	Maximum T_{amb} (°C)	Relative humidity (%)	Accumulated rainfall (mm)	Barometric pressure (hPa)
1788	16.9	11.4	22.4	63	558	954.1

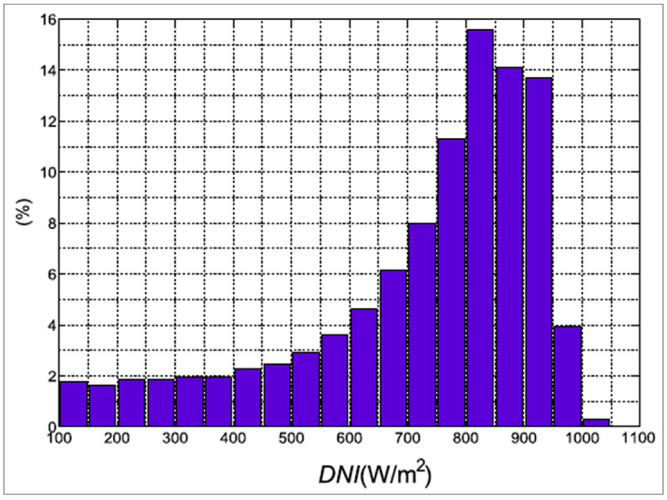

Fig. 3. Total DNI collected in Jaén arranged in different intervals.

been measured from 350 nm up to 1050 nm with a wavelength resolution of approximately 3 nm; therefore, the measurement range of this device determines these wavelength limits.

4. Results and discussion

The spectroradiometers were installed in Jaén which has a high irradiation profile with an approximate annual average daily horizontal global irradiation of 5 kWh·m^{-2} and direct normal irradiation of 6 kWh·m^{-2} [35]. Nevertheless, these values may vary depending on the estimation methods, input data and base years [37]. In Fig. 3, the DNI radiation collected in Jaén during the analysed period (from March 2013 to February 2014), can be observed in percentage terms. It shows that most of the irradiation is collected at high levels of DNI, mainly between 800 and 900 W m^{-2}.

The spectral irradiance results obtained in the periods considered, corresponding to the tracking configurations proposed (DNI tracker, GI tracker and GI fixed), are analysed in detail in the following subsections.

4.1. Spectral irradiance distribution. Characterization

4.1.1. Analysis of APE values and solar irradiation by APE intervals

In this subsection, the spectral irradiance related to several APE intervals is analysed according to the data measured in the selected location. In the following figures, the relative frequency distribution of APE (%) is described, together with the distribution of the collected irradiation (kWh·m^{-2}) for each of the tracking options selected, that is, DNI tracker, GI tracker and GI fixed. In these cases, the results are shown as a fraction of APE, with a class width of 0.02 eV.

The DNI tracker option results are shown in Fig. 4, where it can be observed that both the highest percentage of APE values and the annual solar irradiation were achieved in the 1.82–1.84 eV interval. Around 31% of APE values falls within this range where the direct normal irradiation value raised up to 771 kWh·m^{-2}. Besides, this figure shows that the largest percentages and irradiation figures are distributed between 1.78 eV and 1.86 eV.

If the analysis is focused on the GI tracker configuration, Fig. 5 shows a slight shift to higher APE values. The highest percentage of APE and irradiation figures are located in the range 1.86–1.88 eV, where it is gathered 27% of APE values and 843 kWh·m^{-2} of global irradiation is measured.

Finally, the GI fixed option analysed in Fig. 6 reveals that the highest values are collected in the same interval as the GI tracker (1.86–1.88 eV), but it should be paid notice that they are larger as

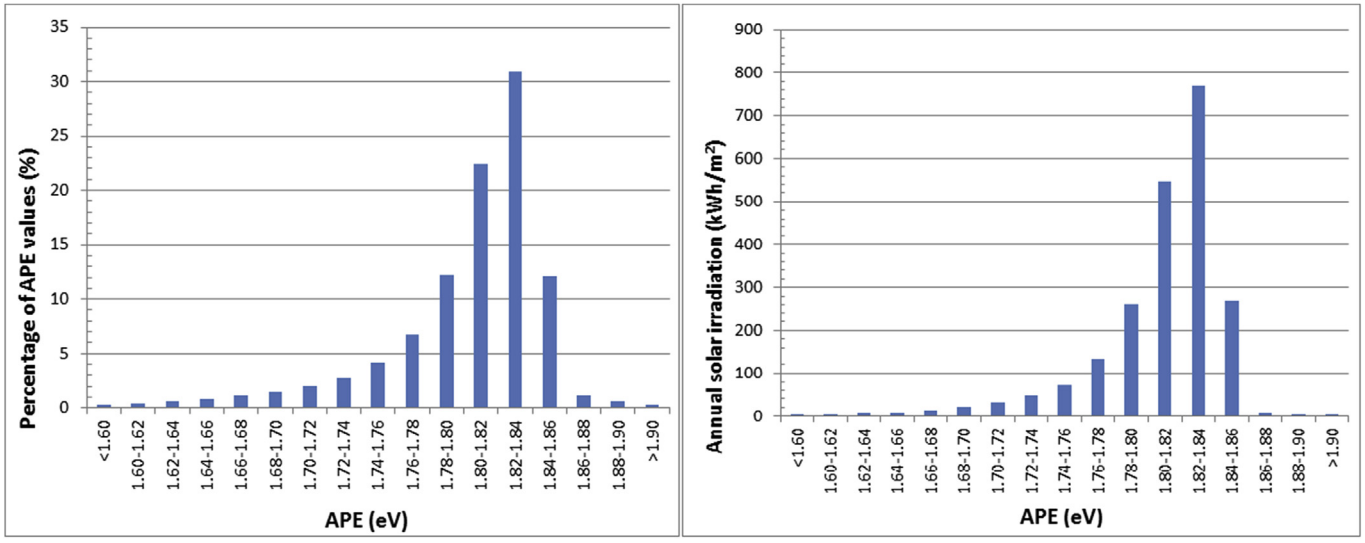

Fig. 4. DNI configuration: Relative frequency and direct normal irradiation distributions as a fraction of APE.

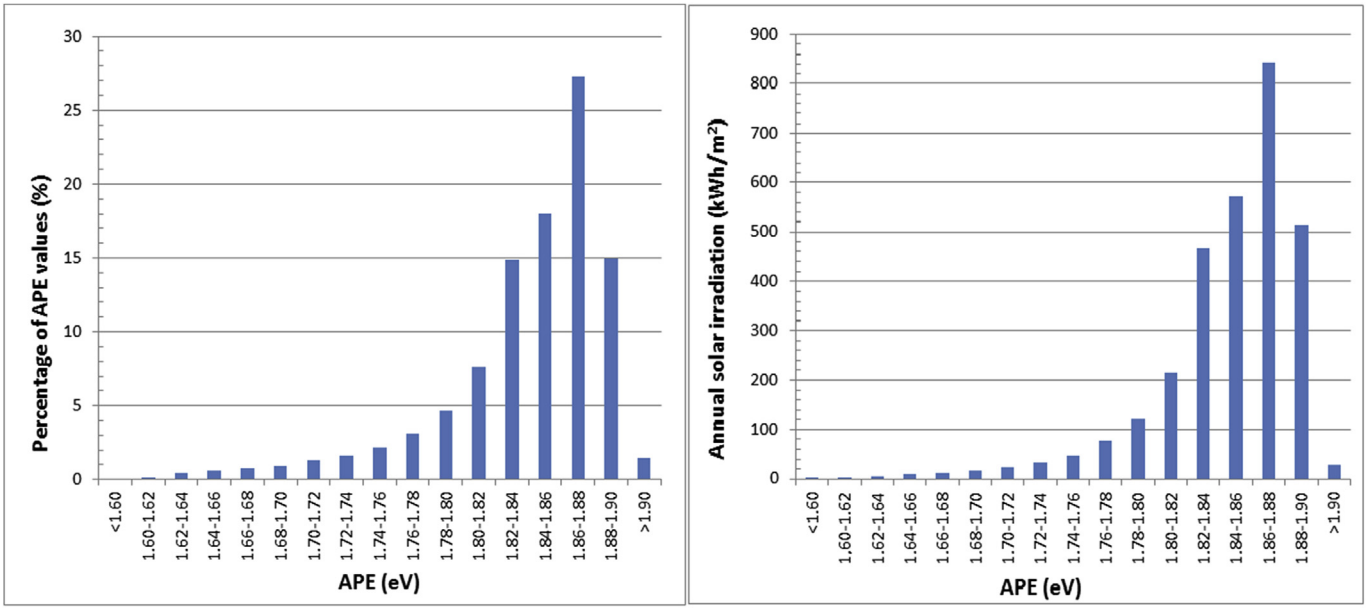

Fig. 5. GI tracker configuration: Relative frequency and global irradiation distributions as a fraction of APE.

49% of APE values and 1143 kWh·m^{-2} of global irradiation is achieve in this interval. Moreover, a big difference between the interval 1.86–1.88 eV and the other ones can be observed. There is a tighter distribution where most data are condensed at higher APE values.

It must be highlighted that higher collected irradiation levels take place in APE classes at which higher relative frequencies occur.

4.1.2. Monthly variation of APE

Once the APE values have been characterized in terms of frequency percentage and annual solar irradiation, an analysis of the monthly variation and their annual mean value for each tracking option should be undertaken. In this direction, Figs. 7–9 provide these values, which have been generated based on approximately 23000 data points measured for each figure.

Fig. 7 shows the maximum, minimum and average monthly APE values for the DNI tracker option in the period analysed (March 2013–February 2014). The maximum APE value was registered in September while the minimum one was obtained in May, resulting 1.95 eV and 1.52 eV respectively. The monthly mean APE values have been averaged for the complete year analysed resulting in an annual mean value of 1.8 eV. For this calculation, Equation (2) has been applied:

$$\overline{APE} = \frac{\sum_{i=1}^{n} APE_i \cdot (G \text{ or } B)_i}{\sum_{i=1}^{n} (G \text{ or } B)_i} \quad (2)$$

On the other hand, Fig. 8 shows the maximum, minimum and average monthly APE results for the GI tracker configuration, whose measurement period analysed is comprised between November 2011 and October 2012. The maximum value reached 2.05 eV, which was recorded in May, whereas the minimum value measured was 1.59 eV (February). In this period and for this tracking configuration, the average annual value of APE was 1.84 eV.

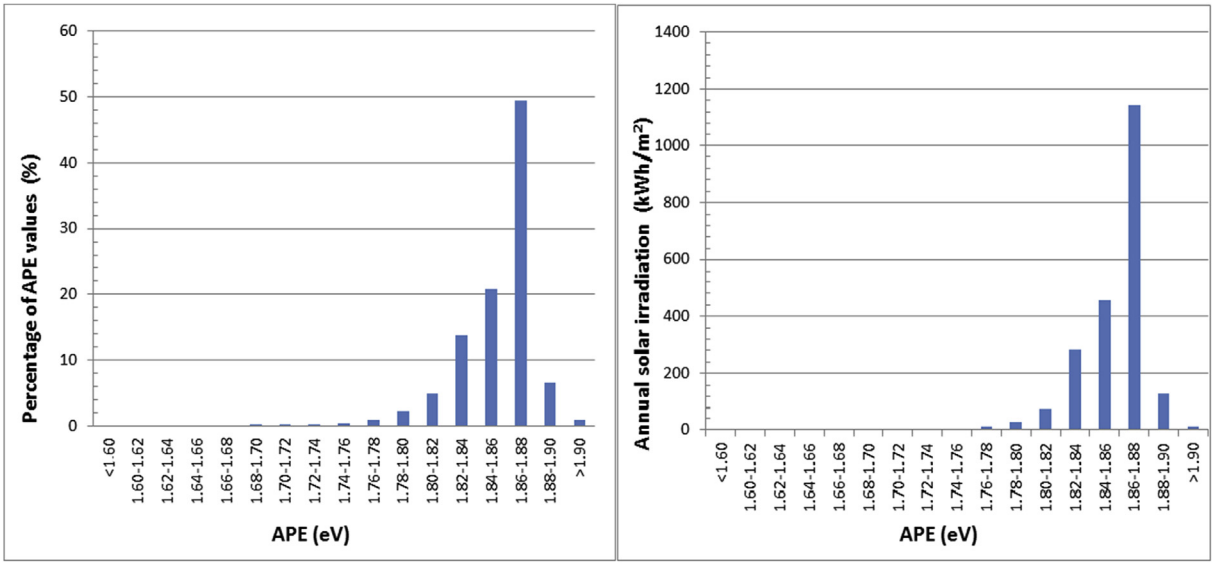

Fig. 6. GI fixed configuration: Relative frequency and global irradiation distributions as a fraction of APE.

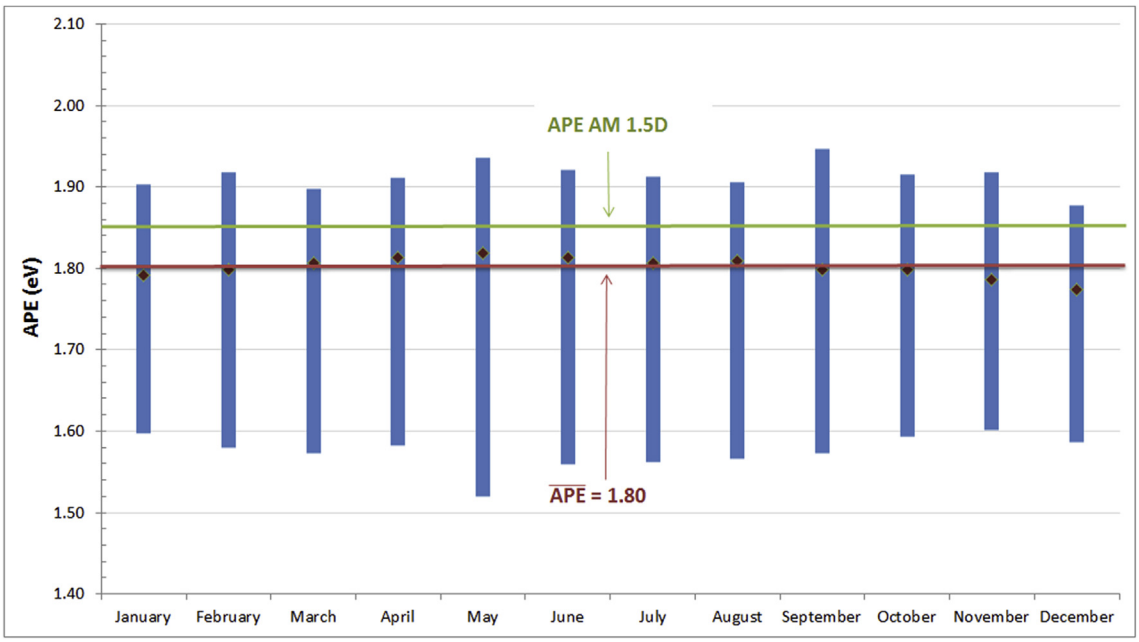

Fig. 7. Maximum, minimum and average monthly APE values for DNI tracker configuration.

Lastly, the GI fixed configuration results showed in Fig. 9 reveal that for the period considered (January 2012–December 2012), the maximum APE value was registered in May, achieving 2.01 eV whereas the minimum value, 1.86 eV, was recorded in February. When averaging the results in an annual term, it is shown that the annual mean value of APE for the GI fixed configuration is 1.86 eV.

Prior to a detailed comparison of the data among the configurations proposed, it is remarkable that the range of variation between maximum and minimum monthly APEs for DNI and GI tracker options is larger meanwhile the monthly differences for GI fixed configuration are smaller.

In this section, the most remarkable result is that the monthly mean value of APE in all three options is between 0.02 and 0.08 eV below the APE mean value for the AM1.5 standard solar spectrum, either global or direct depending on the analysed option. The APE value for the AM 1.5D standard solar spectrum is 1.88 eV, whereas for the AM 1.5G standard solar spectrum is 1.85 eV, so the experimental results exhibits that red-rich spectra prevails in the Southern location chosen (Jaén).

4.2. Spectral irradiance distribution. Comparison

In this section, the results of the three configuration studied in the previous section are inter-compared.

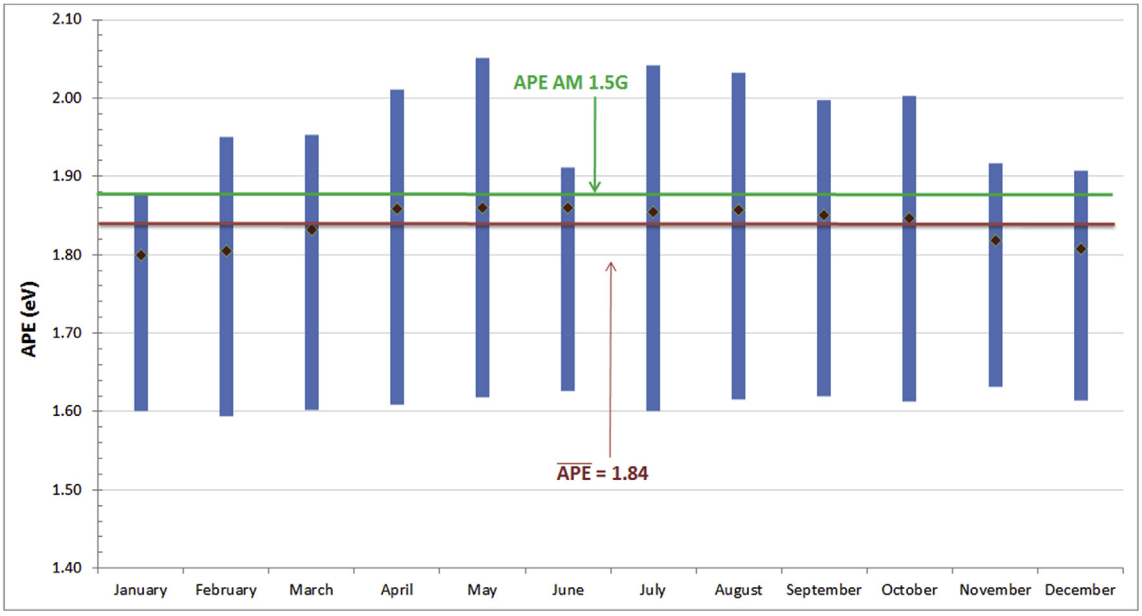

Fig. 8. Maximum, minimum and average monthly APE values for GI tracker configuration.

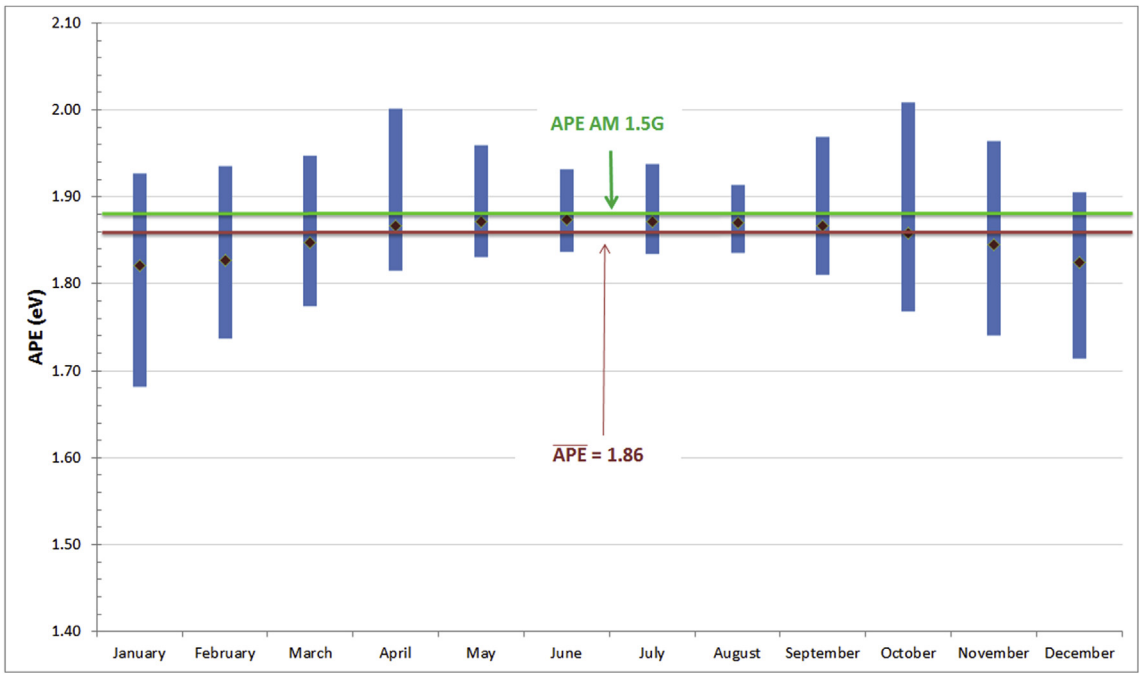

Fig. 9. Maximum, minimum and average monthly APE values for GI fixed configuration.

4.2.1. Analysis of APE values and solar irradiation by APE intervals

It could be distinguished from Figs. 4–6, a slight shift to higher APE values when analysing from DNI and GI tracker options to GI fixed one. This trend is more noticeable when clustering those figures as it is observed in Figs. 10 and 11, where the percentage of APE and irradiation values grouped by APE intervals are shown respectively.

From these figures, it can be seen that the DNI tracker option has most values below 1.84 eV, while the GI ones (tracker and fixed) options are mostly distributed below 1.88 eV, so the increase in the incident angle of the collected sunlight results in a shift in the spectrum towards "blue-rich" area.

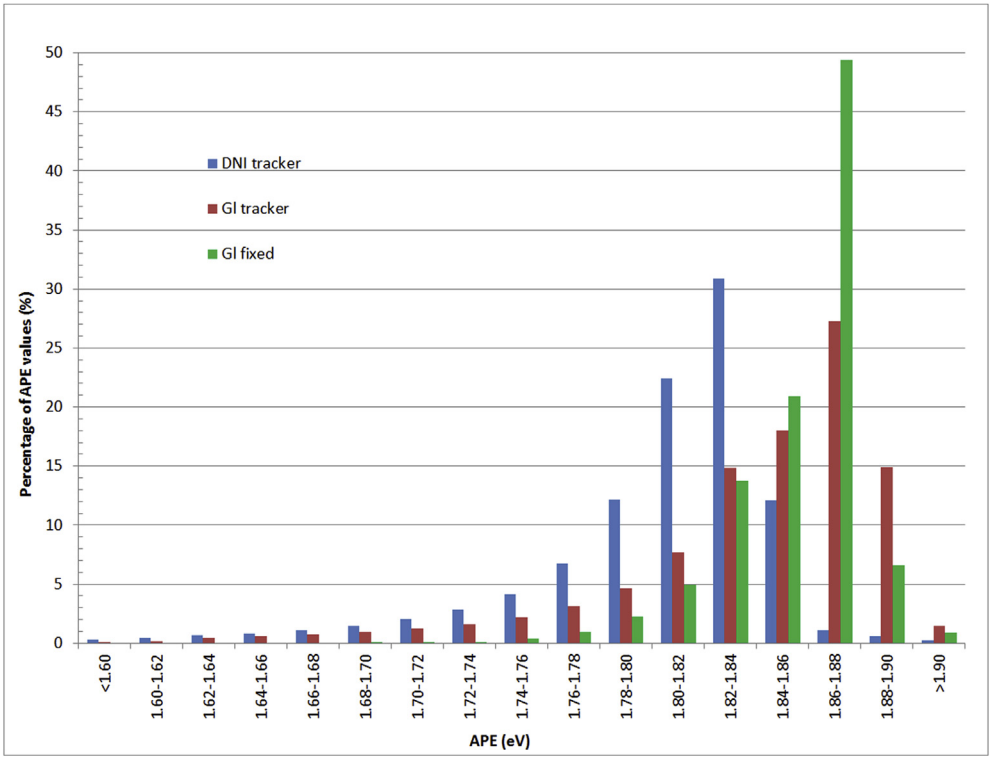

Fig. 10. APE values percentages obtained for the three configurations.

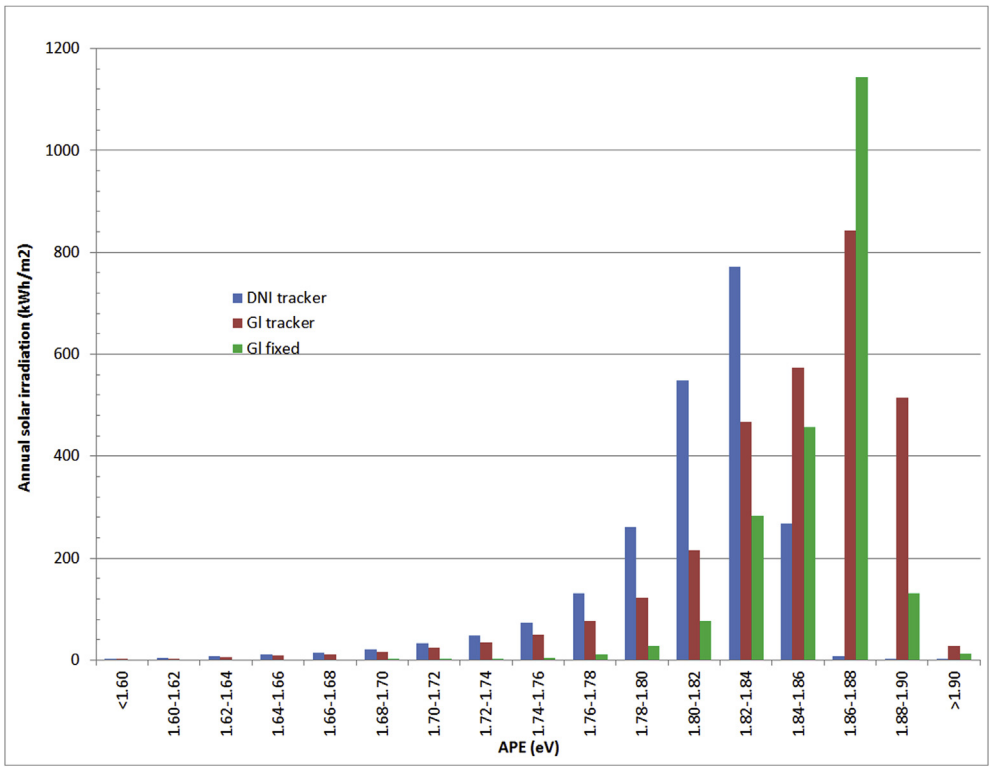

Fig. 11. Irradiation values measured obtained for each configuration.

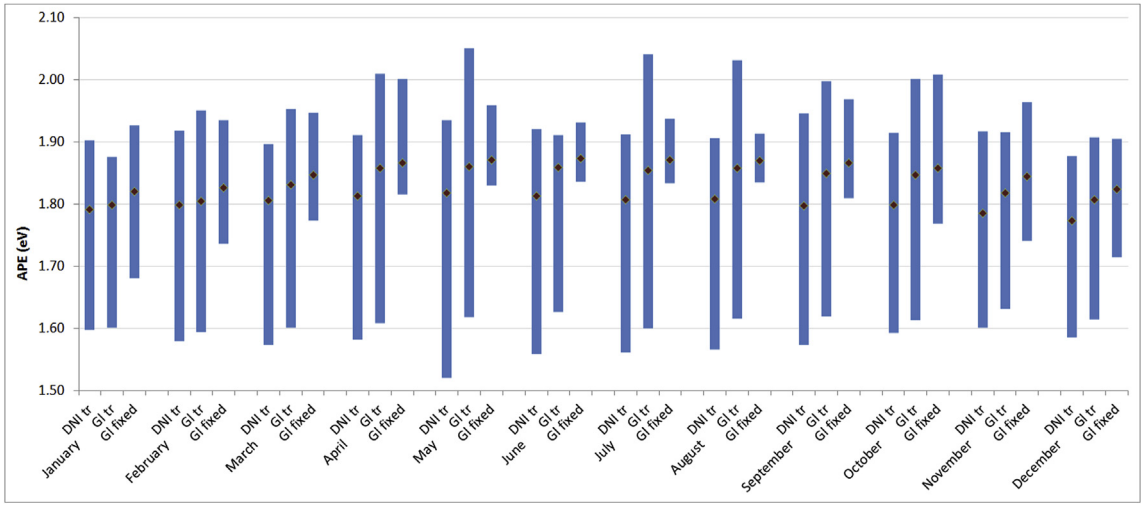

Fig. 12. Maximum, minimum and average monthly APE values for each of the three configurations.

4.2.2. Monthly variation for APE

Likewise the previous section, in the following picture (Fig. 12) there is a combined comparison of the maximum, minimum and average monthly APE values for the three configurations. According to these experimental data, it must be highlighted that the DNI tracker option has lower APE values than the other ones, thus, resulting in a red-shifted spectral measurement. The explanation for this value comes from the fact that when analysing DNI irradiance data versus global ones, the diffuse and albedo component of the irradiance are not taken into account, which would shift the spectrum to the blue region, that is, a more energetic area. Therefore, the solar spectrum for the DNI tracker option is redder and so APE is lower.

Table 2
Average APE normalised to the irradiance value for each of the three configurations analysed.

Option	Average APE normalised to irradiance value
DNI tracker	1.80 eV
GI tracker	1.85 eV
GI fixed	1.86 eV

Finally, if Equation (2) is used to calculate the irradiance-weighted average APE, it can be observed that highest average APE corresponds to GI fixed configuration, followed by a similar value when considering the GI tracker, whereas the lowest level of APE is produced by the DNI tracker option (see Table 2).

4.3. Correlation between spectral distribution and solar irradiance

In order to analyse possible correlations between the spectral distribution and solar irradiance values, there is a comparative hereafter shown in Figs. 13–15.

For each solar spectrum measured, an APE has been calculated and there is an irradiance value, either in global or direct normal terms, which correspond to the APE value calculated. These pairs of values are plotted for each month and similar figure to the ones shown in pictures 13 to 15 are obtained. In this case, an arbitrary month (April) has been chosen, although these results were similar for the rest of months.

If the APE versus direct normal irradiance (DNI) is plotted, the results pictured in Fig. 13 are obtained. For APEs between 1.50 and 1.60 eV, irradiance is always below 500 W m^{-2}. For APEs between 1.60 and 1.70 eV, irradiance is always below 800 W m^{-2}. For APEs above 1.70 eV, irradiances between 500 and 1000 W m^{-2} predominate.

On the other hand, Fig. 14 shows the relationships between APE and global irradiance for the Gl tracker option. In this case, APE values between 1.60 and 1.70 eV correspond to a global irradiance which is always below 700 W m^{-2}. For APEs between 1.70 and 1.80 eV, irradiance is no greater than 1000 W m^{-2}, and those APE values above 1.80 eV, the irradiance is mostly concentrated in the 800–1200 W m^{-2} interval.

Finally, if the global irradiance is analysed in terms of APE for the Gl fixed option, it can be observed (Fig. 15) that most measurements are gathered between 1.80 and 1.90 eV.

It can be noticeable that low values of APE always take place at low levels of irradiance. These specific low irradiance data are related to high values of optical air mass (OAM), which correspond with the early and late hours of the day. Consequently, larger wavelengths (red area) are enhanced. Nevertheless, high values of APE occur at both high and low irradiance levels, therefore high irradiance values imply clear skies in which spectra are shifted to shorter wavelengths, that is, more energetic region (blue area). Likewise, low irradiance levels which take place under overcast conditions lead to “blue-rich” spectra, owing to the absorption by water vapour at longer wavelengths.

5. Conclusions

The results exposed in this paper are particularly important because they provide real spectral measurements and APE values for a sunny inland climate, so that the solar spectrum in this type of climate is characterized. Therefore, it contributes to fill the scarcity of outdoor real data. Additionally, these spectral measurements and APE values are taken for different tracking options, thus this paper additionally provides knowledge about the solar spectrum characterization under different tracking options using APE as indicator.

The immediate conclusion is that all mean values of APE for every month of the three tracking options studied in this document, are below the APE value corresponding to the AM1.5 standard solar spectrum, either considering the global or direct term. It means that red-shifted spectra predominate in the Southern location chosen (Jaén). The range of variation between maximum and minimum APEs for an individual month is much higher for those options which include a tracking mechanism, whereas the variation is not so broaden for fixed ones.

If the results of all the configurations are inter-compared, a similar behaviour has been observed independently the systems studied (with or without tracking mechanism). It is referred to the fact that low values of APE always take place at low irradiance levels, while high values of APE may appear at indistinctly both high and low irradiance levels. High APEs with low irradiance match with cloudy days as a consequence of the “red spectral” absorption of the clouds, thus, resulting in a shift of the spectrum to the blue region. Consequently APE values are higher.

The configuration which covers the direct spectrum has lower APEs than those options which analyse the global spectrum. The explanation for that phenomenon is due to the fact that the direct irradiance does not consider diffuse and albedo components, which

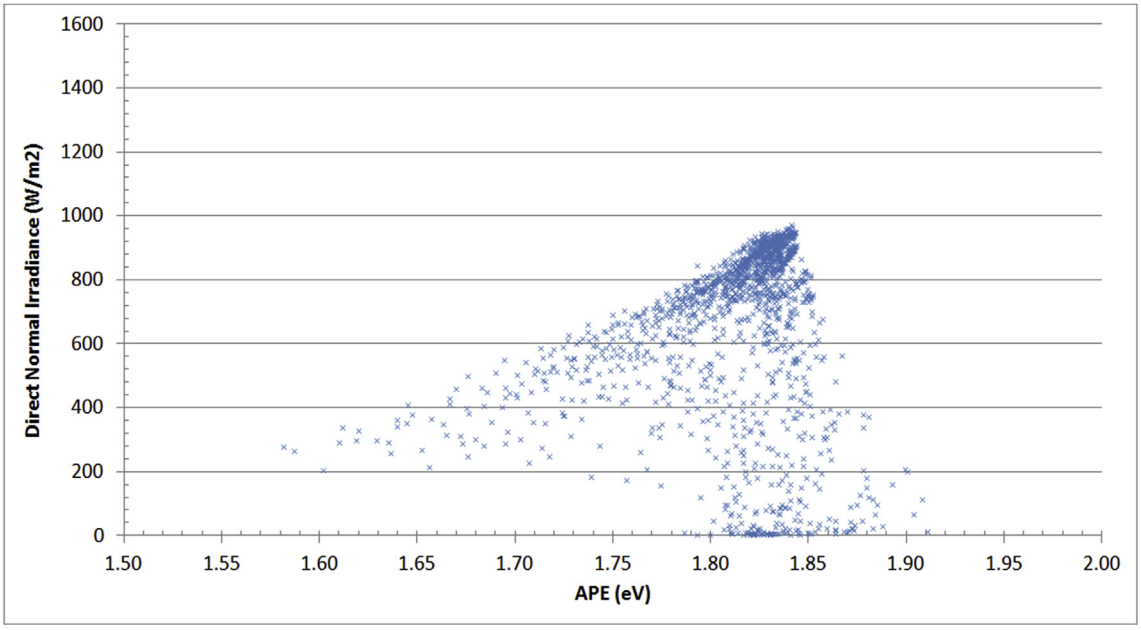

Fig. 13. Direct Normal Irradiance versus APE for the DNI tracker configuration.

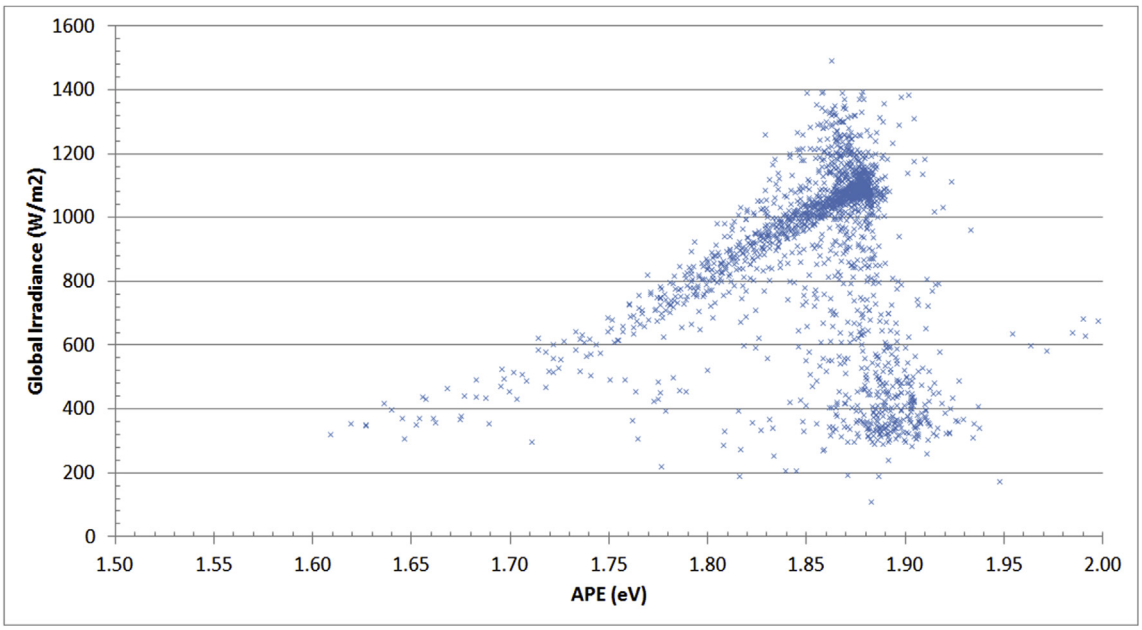

Fig. 14. Global Irradiance versus APE for the GI tracker configuration.

would shift the spectrum to the blue region. This trend has also been corroborated with the average APE normalised to the irradiance values, where the following results were obtained: 1.80 eV for DNI tracker, 1.85 eV for GI tracker and 1.86 eV for GI fixed.

An important conclusion is that the prevailing red-rich GI fixed spectra in Jaén makes this site especially suitable for single junction materials with large absorption band such as CIGS and c-Si.

Furthermore, GI tracker spectra are, on average, slightly redder than GI fixed ones. Consequently, if c-Si modules are used for a certain PV system, spectral gains with 2-axis tracking will be higher than those achieved with a fixed arrangement of such modules.

Finally, concerning CPV technology, APE values of 1.80 for DNI tracker show that the spectra in Jaén can be characterized by low-medium values of precipitable water and a clear atmosphere with very low levels of aerosol optical depth (AOD). So that, the city of Jaén, with a high annual average daily direct normal irradiation of around 6 $kWh \cdot m^{-2}$, is a site especially suitable for the installation of this technology.

As a mayor conclusion, the approach used in this paper could be valuable, mainly to those PV systems based on thin-film technologies and CPV, which in comparison to traditional PV systems based on Silicon, they have been widely proven to be extremely dependent on the variations of the spectrum. Therefore, spectral data based not only on simulations but on real measurements on

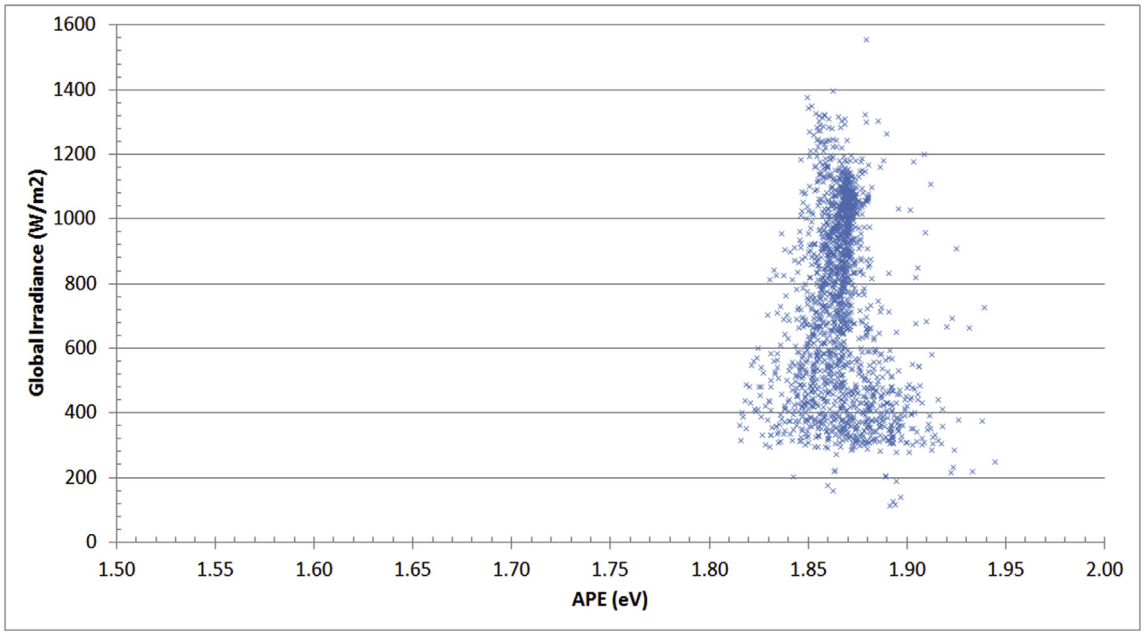

Fig. 15. Global irradiance versus APE for the GI fixed configuration.

the ground could be very clarifying and useful for further scientific works and even for the CPV and Thin-Film industry.

Acknowledgements

This work was supported by the Spanish Science and Innovation Department under the project ENE2009-08302 and by the Department of Science and Innovation of the Regional Government of Andalucía under the project P09-TEP-5045.

Glossary

$\Phi(\lambda)$	spectral photon flux density [$m^{-2}\cdot\mu m^{-1}\cdot s^{-1}$]
λ_1, λ_2	lower and upper wavelength limits [nm]
AM 1.5	Air Mass
AOD	Aerosol Optical Depth
APE	Average Photon Energy
$\overline{APE}$	Annual irradiance weighted average value of APE
CdTe	Cadmium Telluride
CIGS	Copper indium gallium selenide
CPV	Concentrating Photovoltaic
CSP	Concentrated Solar Power
DNI	Direct Normal Irradiance
DNI tracker	Direct Normal solar spectrum on a 2-axis tracking system
$E_\lambda(\lambda)$	spectral in-plane irradiance [$W\cdot m^{-2}\cdot\mu m^{-1}$]
eV	electronvolts
GI	Global Irradiance
GI fixed	Global solar spectrum on a fixed south facing tilted surface
GI tracker	Global solar spectrum on a 2-axis tracking system
OAM	Optical Air Mass
PV	Photovoltaic
Si	Silicon
STC	Standard Testing Conditions
Tamb	Ambient Temperature
UF	Useful Fraction

References

[1] Arnulf Jäger-Waldau, PV Status Report 2014, Ispra, Italy, 2014.
[2] Fraunhofer Institute for Solar Energy Systems ISE, Annual Report 2015/16, Freiburg, Germany, 2015.
[3] T. Minemoto, M. Toda, S. Nagae, M. Gotoh, A. Nakajima, K. Yamamoto, H. Takakura, Y. Hamakawa, Effect of spectral irradiance distribution on the outdoor performance of amorphous Si//thin-film crystalline Si stacked photovoltaic modules, Sol. Energy Mater. Sol. Cells 91 (2–3) (Jan. 2007) 120–122.
[4] C. Sirisamphanwong, N. Ketjoy, C. Sirisamphanwong, The effect of average photon energy and module temperature on performance of photovoltaic module under Thailand's climate condition, Energy Procedia 56 (2014) 359–366.
[5] D.L. Evans, Simplified method for predicting photovoltaic array output, Sol. Energy 27 (6) (1981) 555–560.
[6] G. Nofuentes, J. de la Casa, M. Torres-Ramírez, M. Alonso-Abella, Solar spectral and module temperature influence on the outdoor performance of thin film PV modules deployed on a sunny inland site, Int. J. 2013 (2013) 1–12.
[7] D. Dirnberger, G. Blackburn, B. Müller, C. Reise, On the impact of solar spectral irradiance on the yield of different PV technologies, Sol. Energy Mater. Sol. Cells 132 (Jan. 2015) 431–442.
[8] K. Araki, M. Yamaguchi, Influences of spectrum change to 3-junction concentrator cells, Sol. Energy Mater. Sol. Cells 75 (3–4) (Feb. 2003) 707–714.
[9] S. Senthilarasu, E.F. Fernández, F. Almonacid, T.K. Mallick, Effects of spectral coupling on perovskite solar cells under diverse climatic conditions, Sol. Energy Mater. Sol. Cells 133 (Feb. 2015) 92–98.
[10] C.A. Gueymard, Interdisciplinary applications of a versatile spectral solar irradiance model: a review, Energy 30 (9) (Jul. 2005) 1551–1576.
[11] T.R. Betts, R. Gottschalg, D.G. Infield, Aspire - a tool to investigate spectral effects on PV device performance, in: Proceedings of the 3rd World Conference on Photovoltaic Energy Conversion, vol. C, 2003, pp. 2182–2185.
[12] P. Ricchiazzi, S. Yang, C. Gautier, D. Sowle, SBDART: a research and teaching software tool for plane-parallel radiative transfer in the Earth's atmosphere, Bull. Am. Meteorol. Soc. 79 (10) (1998) 2101–2114.
[13] S.A. Clough, M.W. Shephard, E.J. Mlawer, J.S. Delamere, M.J. Iacono, K. Cady-Pereira, S. Boukabara, P.D. Brown, "Atmospheric radiative transfer modeling: a summary of the AER codes, J. Quant. Spectrosc. Radiat. Transf. 91 (2) (Mar. 2005) 233–244.
[14] S. Nann, C. Riordan, Solar spectral irradiance under clear and cloudy skies: measurements and a semiempirical model, J. Appl. Meteorol. 30 (4) (Apr. 1991) 447–462.
[15] M. Kocifaj, Unified model of radiance patterns under arbitrary sky conditions, Sol. Energy 115 (2015) 40–51.
[16] M. Kocifaj, Angular distribution of scattered radiation under broken cloud arrays: an approximation of successive orders of scattering, Sol. Energy 86 (12) (2012) 3575–3586.
[17] M. Torres-Ramírez, D. Elizondo, B. García-Domingo, G. Nofuentes, D.L. Talavera, Modelling the spectral irradiance distribution in sunny inland locations using an ANN-based methodology, Energy 86 (Jun. 2015) 323–334.
[18] R. Gottschalg, T.R. Betts, D.G. Infield, M.J. Kearney, Experimental investigation of spectral effects on amorphous silicon solar cells in outdoor operation, in: Conference Record of the IEEE Photovoltaic Specialists Conference, 2002, pp. 1138–1141.
[19] C. Jardine, T. Betts, R. Gottschlg, D.G. Infield, K. Lane, Influence of spectral effects on the performance of multijunction amorphous silicon cells, in: 17th Eur. Photovolt. Sol. Energy Conf., vol. 44, 2002, pp. 2–5 no. 0.
[20] G. Nofuentes, B. García-Domingo, J.V. Muñoz, F. Chenlo, Analysis of the dependence of the spectral factor of some PV technologies on the solar spectrum distribution, Appl. Energy 113 (Jan. 2014) 302–309.
[21] N. Martín, J.M. Ruiz, New method for the spectral characterization of PV modules, Prog. Photovolt. Res. Appl. 7 (4) (1999) 299–310.
[22] International Electrotechnical Commission, IEC 60904–3:2016. Photovoltaic Devices - Part 3: Measurement Principles for Terrestrial Photovoltaic (PV) Solar Devices with Reference Spectral Irradiance Data, 2016.
[23] ASTM International, ASTM G173–03(2012), Standard Tables for Reference Solar Spectral Irradiances: Direct Normal and Hemispherical on 37° Tilted Surface, ASTM International, 2012.
[24] J. Chantana, S. Ueno, Y. Ota, K. Nishioka, T. Minemoto, Uniqueness verification of direct solar spectral index for estimating outdoor performance of concentrator photovoltaic systems, Renew. Energy 75 (Mar. 2015) 762–766.
[25] T. Minemoto, Y. Nakada, H. Takahashi, H. Takakura, Uniqueness verification of solar spectrum index of average photon energy for evaluating outdoor performance of photovoltaic modules, Sol. Energy 83 (8) (2009) 1294–1299.
[26] R. Gottschalg, D.G. Infield, M.J. Kearney, Experimental study of variations of the solar spectrum of relevance to thin film solar cells, Sol. Energy Mater. Sol. Cells 79 (4) (Sep. 2003) 527–537.
[27] C. Cornaro, A. Andreotti, Influence of Average Photon Energy index on solar irradiance characteristics and outdoor performance of photovoltaic modules, Prog. Photovolt. Res. Appl. 21 (5) (Apr. 2012) p. n/a–n/a.
[28] N. Kataoka, S. Yoshida, S. Ueno, T. Minemoto, Evaluation of solar spectral irradiance distribution using an index from a limited range of the solar spectrum, Curr. Appl. Phys. 14 (5) (May 2014) 731–737.
[29] C.A. Gueymard, Daily spectral effects on concentrating PV solar cells as affected by realistic aerosol optical depth and other atmospheric conditions, in: Proceedings of SPIE - the International Society for Optical Engineering, vol. 7410, 2009, 741007–741007–14.
[30] R. Hofmann, M. Vanicek, P. Haselhuhn, Is the average photon energy (APE) a suitable measure to describe the uniqueness of solar spectra?Title, in: 29th European Photovoltaic Solar Energy Conference and Exhibition, 2014, pp. 3461–3466.
[31] M. Alonso-Abella, F. Chenlo, G. Nofuentes, M. Torres-Ramírez, Analysis of spectral effects on the energy yield of different PV (photovoltaic) technologies: the case of four specific sites, Energy 67 (Apr. 2014) 435–443.
[32] National Institute of Meteorology, Guía resumida del clima en España (1981-2010), 2010.
[33] G. Nofuentes, M. Alonso-Abella, J.V. Muñoz, B. García-Domingo, M. Fuentes, J. De la Casa, F. Chenlo, Influence of spectral irradiance distribution and module temperature on the outdoor performance of some thin film PV module technologies, in: Proceedings of the 26th European Photovoltaic Solar Energy Conference, 2011, pp. 3351–3354.
[34] G. Nofuentes, B. García-Domingo, M. Fuentes, R. Moreno, C. Cañete, M. Sidrach-de-Cardona, M.A. Alonso, F. Chenlo, Comparative analysis of the effects of spectrum and module temperature on the performance of thin film modules on different sites, in: Proceedings of the 26th European Photovoltaic Solar Energy Conference, 2012.
[35] Joint Research Center. European Union, Photovoltaic Geographical Information System - Interactive Maps, [Online]. Available: http://re.jrc.ec.europa.eu/pvgis/apps4/pvest.php. [Accessed 06 May 2016].
[36] Deutsche Gesellschaft für Sonnenenergie DGS, Planning and Installing Photovoltaic Systems. A Guide for Installers, Architects and Engineers, third ed., Routledge, 2013.
[37] P.J. Pérez-Higueras, P. Rodrigo, E.F. Fernández, F. Almonacid, L. Hontoria, A simplified method for estimating direct normal solar irradiation from global horizontal irradiation useful for CPV applications, Renew. Sustain. Energy Rev. 16 (8) (Oct. 2012) 5529–5534.